C_2H_5OH and LPG sensing properties of α-Fe_2O_3 microflowers prepared by hydrothermal route

- **Luong Huu Phuoc** *
- **Do Duc Tho**
- **Nguyen Dac Dien**
- **Vu Xuan Hien**
- **Dang Duc Vuong**

School of Engineering Physics, Hanoi University of Science and Technology, Hanoi, Vietnam

(Manuscript Received on December 16th, 2015, Manuscript Revised July 19th, 2016)

ABSTRACT

The flower-like micron-structure of α-Fe_2O_3 was synthesized via hydrothermal treatment at 140 ℃ for 24 h using $Fe(NO_3)_3.9H_2O$ and Na_2SO_4 as the precursors. A thin film constructed by the as-prepared material was created by spin coating technique. The structure, morphology, and composition of the samples were characterized by X-ray diffraction (XRD), field emission scanning electron microscopy (FESEM). The α-Fe_2O_3 microflowers (MFs) with average diameter of several micrometers are assembled of nanorods which possess average diameter and length of 40 nm and hundred nm, respectively. The gas sensing properties of α-Fe_2O_3 film were tested with ethanol (C_2H_5OH) and liquefied petroleum gas (LPG) at the operating temperatures of 225–400 °C. The sensor response of the α-Fe_2O_3 film reached highest sensitivity to C_2H_5OH and LPG at 275 ℃ and 350 °C, respectively. The thin film exhibited higher sensitivity and lower working temperature to C_2H_5OH than those to LPG. The film can detect minimum concentration of 250 ppm C_2H_5OH. The response time of the film to C_2H_5OH is approximately 30 s.

Keywords: *α-Fe_2O_3, gas sensor, microflower, nanorod, hydrothermal.*

1. INTRODUCTION

Hematite (α-Fe_2O_3) is the most stable iron oxide under ambient conditions which behaves as an n-type semiconducting material with band gap of 2.2 eV [1]. It is frequently applied as semiconducting material, dielectric material, magnetic material, sensitive material and catalyst, etc. [2-6]. In recent years, much effort has been focused on the fabrication of nanostructure materials with a desired size, morphology and porosity, owing to their special electrical, optical, magnetic, and

physical/chemical properties that are superior to those bulk materials [7-10]. Stimulated by both the promising applications of iron oxide and the novel properties of nanoscale materials, many scientists have synthesized α-Fe_2O_3 nanostructured materials in various geometrical morphologies such as nanotubes [8], nanoparticles [11], nanowires and nanobelts [12], nanorods [1, 10, 13], nanocubes, sea urchin-like [14], nanoplates [15], etc. Ferric oxide has been prepared by liquid-phase deposition method (LPD) [16], plasma enhanced chemical vapor deposition (PECVD) [17], ion-sputtering [18], ultrasonic spray pyrolysis [19], sol-gel route [2], hydrothermal method [1, 11, 13, 14], etc. Among those methods, hydrothermal treatment is a simple and reliable method for synthesizing nanostructures with designed chemical components and controlled morphologies. Recently, three-dimensional (3D) superstructures assembled with one-dimensional nanorods have attracted much attention due to their higher specific surface area [20].

In this study, we report a facile route to synthesize α-Fe_2O_3 MFs without any surfactant and template via a low temperature (140 °C) hydrothermal approach. The material can be fabricated with large scale and good reproducibility. Besides, the ethanol and LPG sensing characteristics of α-Fe_2O_3 film are also investigated. The results indicated that the sensor response of the α-Fe_2O_3 film reached highest sensitivity to ethanol vapor and LPG at operating temperature of 275 °C and 350 °C, respectively.

2. EXPERIMENTAL

The preparation process of flower-like α-Fe_2O_3 nanostructures is introduced in Fig.1. In a typical synthesis, 100 ml 0.075 M sodium sulfate (Na_2SO_4) solution was added to 100 ml 0.075 M iron (III) nitrate ($Fe(NO_3)_3$) solution. After stirring for 30 min, 10 ml deionized water was added to form a homogeneous solution. The mixed solution was sealed into a Teflon-lined stainless steel autoclave of 50 ml capacity and heated at 140 °C for 24 h. After treatment, the autoclave was cooled to room temperature naturally. The red-brown powder was isolated by centrifugation, washed by deionized water and absolute ethanol several times, and finally dried at 80 °C for 24 h in air. The obtained powder was then characterized by XRD (Bruker D8 Advance X-ray diffractometer, Germany) and scanning electron microscopy (Hitachi S4800, Japan). The α-Fe_2O_3 powder was mixed and grinded with water and PEG to form a gas-sensing paste. The α-Fe_2O_3 material was coated on silicon substrate deposited interdigitated platinum electrodes. In order to improve their stability and repeatability, the gas sensor was annealed at 600 °C for 2 h in air. The gas sensing properties of α-Fe_2O_3 film were tested to C_2H_5OH (250-2000 ppm) and LPG (2500-10000 ppm) at operating temperatures of 225-400 °C.

3. RESULTS AND DISCUSSION

In order to identify whether there is any influence of thermal treatment at 600 °C for 2 h on morphologies and crystal structures of α-Fe_2O_3 mircroflowers (MFs), we measured XRD spectra and took the SEM images of the α-Fe_2O_3 MRs before and after annealing, and these results are demonstrated in Figs. 2 and 3. The main diffraction peaks of the freshly-obtained Fe_2O_3 MRs can be well indexed to a rhombohedral Fe_2O_3 with lattice parameters of a=b=5.0016 Å, c=13.6202 Å, $\alpha=\beta=90°$, $\gamma=120°$, the space group is R-3c (Fig. 2a). Fig. 2b shows the X-ray diffraction (XRD) pattern of the obtained α-Fe_2O_3 after annealing at 600 °C for 2 h. All the

reflection peaks in the XRD pattern are indexed to the single crystal of hexagonal structure of Fe_2O_3 with lattice constants of a=b=5.038 Å, c=13.772 Å and α=β=90°, γ=120°, the space group is R32/c (JCPDS Card No. 33-0664). Thus, the crystal structure of Fe_2O_3 nanorods transfers from rhombohedral before annealing into hexagonal phase after annealing. No further peaks of another phases was observed, suggesting that the product was high purity. The strong and narrow diffraction peaks observed in the pattern indicate that the material possesses a good crystallinity. In the XRD pattern, the (104) diffraction peak has the strongest reflection, indicating that the (104) is the preferential growth plane of the nanorods. The crystallite size of Fe_2O_3 nanorods are estimated using the Scherrer equation based on the (104) peak, and it is found to be around 30 nm before and after annealing.

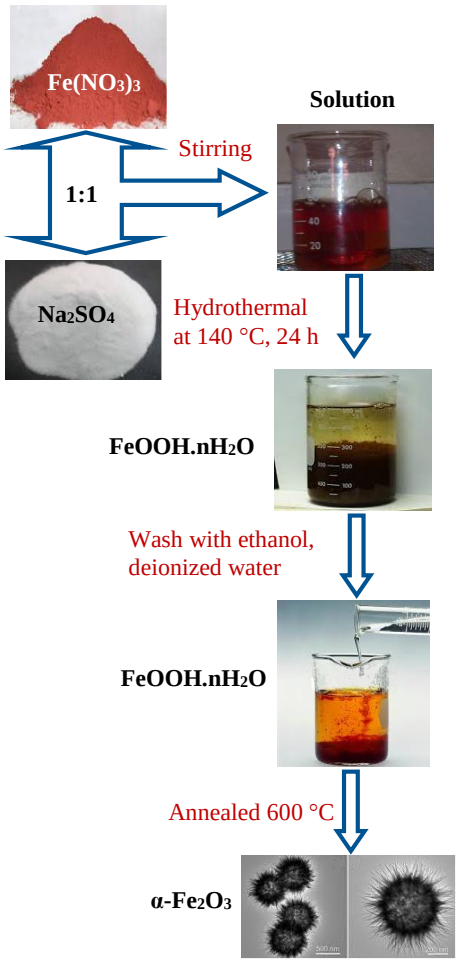

Figure 1. Scheme of α-Fe_2O_3 synthesis.

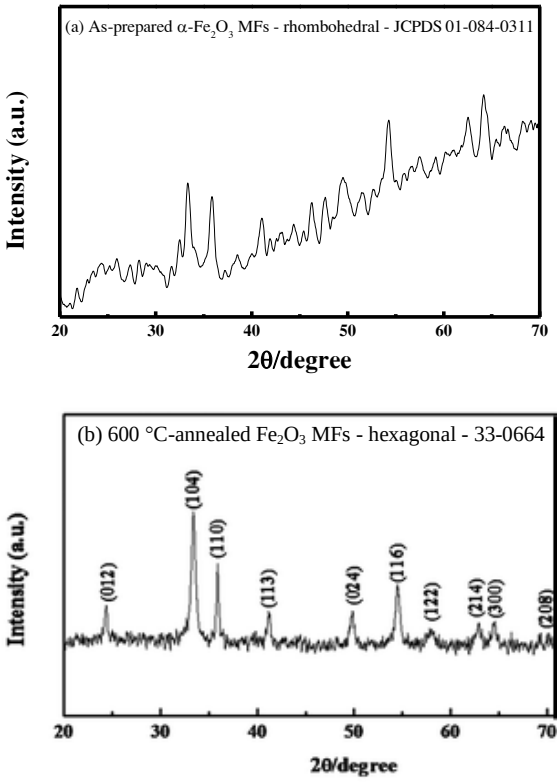

Figure 2. XRD pattern of as-prepared (a) α-Fe_2O_3 microflowers and after annealing at 600 °C for 2 h (b).

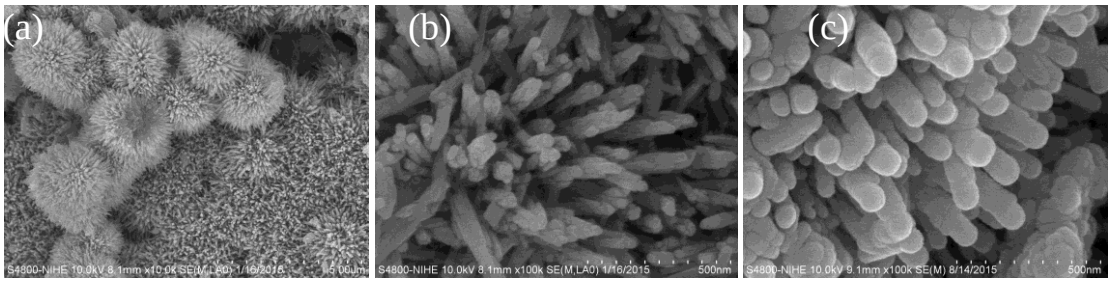

Figure 3. SEM images of as-prepared α-Fe_2O_3 MFs with magnification of 10k (a), 100k (b) and 600 °C-annealed α-Fe_2O_3 MFs with magnification of 100k (c).

The SEM image of the as-prepared sample at magnification of 10k (or ×10000 times) in Fig. 3a shows the microflowers with diameters of 2-3 μm. The microflowers are constructed by wrapped layer of oriented nanorods with diameters of 30–50 nm and lengths of 200–300 nm (Fig. 3b). It can be seen that the α-Fe_2O_3 nanorods are arranged in an orderly fashion. Fig. 3c shows the SEM image of the sample after heat treatment at 600 °C for 2 h. It was observed that the rod-like morphology was maintained, both diameter and length of the nanorods were similar to those of as-prepared product but the rod surface seems smoother.

Figure 4 shows the gas-sensing characteristics of the α-Fe_2O_3 MFs in response to C_2H_5OH. It is known that the sensing characteristic of α-Fe_2O_3 for a special gas is usually dependent on the temperature, so parallel experiments were carried out in the range of 225–325 °C to optimize the proper working temperature of the sensor. As is shown in Fig. 4a, the results indicated that sensor showed the highest response to C_2H_5OH at 275 °C. Regarding to the complex morphology, the thin film exhibits surface roughness which may provide many sites to adsorb the gas molecules, therefore enhances the sensitive properties.

It is generally accepted that the change in resistance is mainly caused by the adsorption and desorption of gas molecules on the surface of the sensing structure [2]. It is possibly related to the chemical reaction kinetics between gas molecules and oxygen ions adsorbed on the surface of the α-Fe_2O_3 superstructures. The relatively looser bundle aggregates can act as gas diffusion channels making the diffusion much easier. The surface-to-volume ratio is relatively high as a result of small diameter of nanorods which enables the gases to access all surfaces of the nanorods contained in the sensing unit. Thus, it is reasonable to believe that sensor made with aligned α-Fe_2O_3 nanorods should have enhanced sensitivity. The response of the sensor based on the porous flower-like α-Fe_2O_3 nanostructures is much higher than that of the α-Fe_2O_3 nanoparticles under the same condition [7] because the porous flower-like nanostructure may possess high surface area which can provide more adsorption-desorption sites for gas molecules compared to that of the nanoparticles. The pseudo-cubic shaped α-Fe_2O_3 particles with the mean size of about 58 nm showed high sensitivity toward C_2H_5OH. Its response to 50 ppm C_2H_5OH at room temperature was 19 [2]. The response of α-Fe_2O_3 nanotubes to 50 ppm

C_2H_5OH at room temperature was 26, about five times greater than that of the α-Fe_2O_3 nanoparticles [8]. The response of the hollow sea urchin-like α-Fe_2O_3 nanostructures to 42 ppm ethanol at 350 °C was 7.2, which was excess twice that of the α-Fe_2O_3 nanocubes [14]. The response of porous α-Fe_2O_3 nanorods to 1000 ppm C_2H_5OH at 250 °C was 175, which was almost several decade times greater than that of α-Fe_2O_3 nanoparticles under the same ethanol concentration [10].

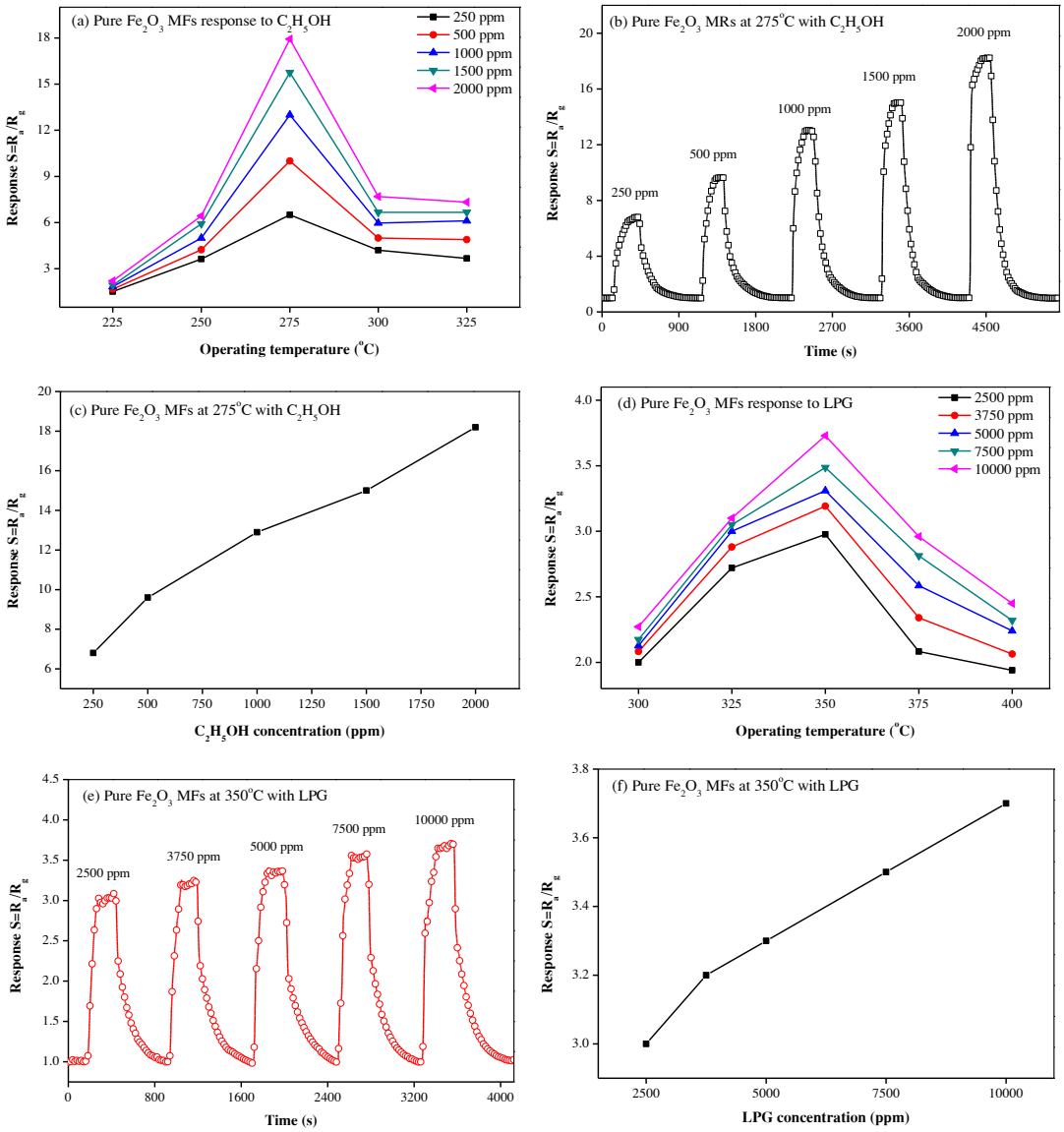

Figure 4. The gas sensing response towards ethanol vapor (a, b, c) and LPG (d, e, f) of pure Fe_2O_3 MFs based sensor.

The chemical reaction rate is slow at lower temperature, leading to a lower response of the sensor. When the operating temperature is high (above 275 °C), desorption process becomes dominant, higher temperature hampers the diffusion of tested gases towards the sensing surface resulting in lowering the diffusion length, leading to reducing of response to ethanol. We thus select 275 °C as the proper working temperature to proceed with the subsequent detections. Fig. 4b illustrates a typical response-recovery characteristic of the sensor based on the porous flower-like α-Fe_2O_3 microstructure to C_2H_5OH with concentrations of 250, 500, 1000, 1500 and 2000 ppm at 275 °C. It can be seen that the response of the sensor increases dramatically with the increase in the ethanol concentration and the highest response is 18 to 2000 ppm ethanol. After several cycles, the resistance of the sensor can recover its initial states, which indicates that the sensor has good reversibility.

Fig. 4c is the plot of sensitivity versus the concentration of C_2H_5OH. The sensitivity increases linearly to the ethanol concentration from 250 to 2000 ppm. The linear relationship between the sensitivity and the ethanol concentration was also observed in the previous reports [2]. The response and recovery times towards 2000 ppm C_2H_5OH are 30 s and 460 s, respectively. Such behavior can be understood by considering the dependence of oxygen adsorption on the operating temperature of the sensor. In the ambience air, the state of oxygen adsorbed on the surface of the material undergoes the following reactions. Oxygen in air is adsorbed onto material surface:

$$O_2(gas) \leftrightarrow O_2(ads) \quad (1)$$

Then, the adsorbed oxygen changes to ion O_2^- following the reaction:

$$O_2(ads) + e^- \leftrightarrow O_2^-(ads) \quad (2)$$

At high temperature, the ions O_2^- change to ions O^-:

$$O_2^-(ads) + e^- \leftrightarrow 2O^-(ads) \quad (3)$$

where (gas) and (ads) denote gas phase and adsorbed species. The oxygen species capture electrons from the material, leading a decrease in electron concentration. When the target gas was injected in the test chamber and reacted with the adsorbed oxygen, electrons traped by the adsorptive states can be released into the conduction band, which resulted in a decrease in sensor resistance. Ethanol reacts with the adsorbed oxygen according to following reaction:

$$C_2H_5OH + 6O^- \rightarrow 2CO_2 + 3H_2O + 6e^- \quad (4)$$

In Fig. 4d, we examine the sensitivity to LPG and the results show that the optimal operating temperature obtained is different from the result shown in Figure 4a. In this experiment, the sensitivity of the sensor increases with increasing operating temperature and reaches its maximum at 350 °C. The maximum response to 10000 ppm LPG at 350 °C is only 3.8, which is about five times lower than that to 2000 ppm ethanol. This behavior may relate to the differences of electron donating ability between C_2H_5OH and LPG, in which C_2H_5OH possesses a higher value due to the high electronegativity of carbon atom comparing with lower electronegativity of oxygen atom. The overall

reaction of LPG molecules comprising C_nH_{2n+2} with the ionic oxygen species can be expressed by:

$$C_nH_{2n+2} + 2O^- \rightarrow H_2O + C_nH_{2n}O^- + e^- \quad (5)$$

Fig. 4f shows the linear relationship between the sensitivity and the LPG concentration of α-Fe_2O_3 MFs. The response and recovery times of the thin film to 10000 ppm LPG are 30 s and 335 s, respectively. It means that this film performs quick response and long recovery duration toward both ethanol and LPG. Furthermore, it is found in the sensing output that the measurement circle is well repeatable without major change in the baseline resistance.

4. CONCLUSION

In summary, flower-like α-Fe_2O_3 microstructures were synthesized by a simple hydrothermal treatment at 140 °C for 24 h. The α-Fe_2O_3 MFs were composed of regular nanorods with average diameter of 40 nm and average length of hundreds nm. Furthermore, the gas-sensing measurements demonstrated that the sensors based on the porous flower-like α-Fe_2O_3 exhibited good sensitivity to C_2H_5OH. The sensor response was 18 towards 2000 ppm of C_2H_5OH at 275 °C. The sensor response to 10000 ppm LPG was 3.8 at 350 °C. This sensor showed a linear, stable and reproducible response to C_2H_5OH in the range of 250–2000 ppm, without significant baseline resistance shift during the test. Furthermore, it exhibits quick response to the C_2H_5OH (30 s).

ACKNOWLEDGMENT

The authors gratefully acknowledge financial support from the National Foundation for Science and Technology Development of Vietnam (NAFOSTED) under grant number 103.99-2015.18.

Tính chất nhạy khí C_2H_5OH và LPG của hoa micro α-Fe_2O_3 chế tạo bằng phương pháp thủy nhiệt

- **Lương Hữu Phước**
- **Đỗ Đức Thọ**
- **Nguyễn Đắc Diện**
- **Vũ Xuân Hiền**
- **Đặng Đức Vượng**

Viện Vật lý kỹ thuật, Đại học Bách khoa Hà Nội

TÓM TẮT

Cấu trúc micro hình hoa α-Fe_2O_3 được tổng hợp bằng xử lí thủy nhiệt ở 140 ℃ trong 24 h sử dụng tiền chất $Fe(NO_3)_3.9H_2O$ và Na_2SO_4. Màng mỏng tạo bởi vật liệu này được tạo bằng kĩ thuật quay phủ. Cấu trúc, hình thái và thành phần của mẫu được xác định bởi giản đồ nhiễu xạ tia X (XRD), hiển vi điện tử quét phát xạ trường (FESEM). Hoa micro α-Fe_2O_3 có đường kính trung bình khoảng vài μm được sắp xếp bởi các thanh nano có đường kính trung bình khoảng 40 nm và chiều dài hàng trăm nm. Tính chất nhạy khí của màng α-Fe_2O_3 được kiểm tra với hơi ethanol (C_2H_5OH) và khí ga hóa lỏng (LPG) ở nhiệt độ làm việc trong khoảng 225 đến 400 ℃. Độ đáp ứng của màng α-Fe_2O_3 đạt cực đại với C_2H_5OH và LPG tương ứng ở 275 ℃ và 350 ℃. Mẫu cho thấy độ nhạy cao hơn và nhiệt độ làm việc thấp hơn với C_2H_5OH so với LPG. Màng có thể phát hiện nồng độ nhỏ nhất của C_2H_5OH là 250 ppm. Thời gian đáp ứng của màng với C_2H_5OH xấp xỉ 30 s.

Từ khóa:

REFERENCES

[1]. Dang Duc Vuong, Khuc Quang Trung, Nguyen Hoang Hung, Nguyen Van Hieu, Nguyen Duc Chien, Facile preparation of large-scale α-Fe_2O_3 nanorod/SnO_2 nanorod composites and their LPG-sensing properties, *Journal of Alloys and Compounds* 599 (2014) 195–201.

[2]. Lihua Huo, Qiang Li, Hui Zhao, Lijun Yu, Shan Gao, Jinggui Zhao, Sol–gel route to pseudocubic shaped α-Fe_2O_3 alcohol sensor: preparation and characterization, *Sensors and Actuators B* 107 (2005) 915–920.

[3]. M. Vasquez Mansilla, R. Zysler, D. Fiorani, L. Suber, Annealing effects on magnetic properties of acicular hematite nanoparticles, *Physica B* 320 (2002) 206–209.

[4]. C.C. Chai, J. Peng, B.P. Yan, Characterization of α- Fe_2O_3 thin films deposited by atmospheric pressure CVD onto alumina substrates, *Sensors and Actuators B* 34 (1996) 412–416.

[5]. Baolong Yu, Congshan Zhu, Fuxi Gan, Large nonlinear optical properties of Fe_2O_3 nanoparticles, *Physica E* 8 (2000) 360–364.

[6]. P. Chauhan, S.K. Trikha, S. Annapoorni, Humidity-sensing properties of nanocrystalline hematite thin films prepared by sol–gel processing, *Thin Solid Films* 346 (1999) 266–268.

[7]. Wei Yan, Huiqing Fan, Yuchun Zhai, Chao Yang, Pengrong Ren, Limei Huang, Low temperature solution-based synthesis of porous flower-like α-Fe_2O_3 superstructures and their excellent gas-sensing properties, *Sensors and Actuators B* 160 (2011) 1372–1379.

[8]. Jun Chen, Lina Xu, Weiyang Li, Xinglong Gou, α-Fe_2O_3 nanotubes in gas sensor and lithium-ion battery applications, *Advanced Materials* 17 (2005) 582–586.

[9]. An-Min Cao, Jin-Song Hu, Han-Pu Liang, Wei-Guo Song, Li-Jun Wan, Xiu-Li He, Xiao-Guang Gao, Shan-Hong Xia, Hierarchically structured cobalt oxide (Co_3O_4): the morphology control and its potential in sensors, *Journal of Physical Chemistry B* 110 (2006) 15858–15863.

[10]. Yan Wang, Jianliang Cao, Shurong Wang, Xianzhi Guo, Jun Zhang, Huijuan Xia, Shoumin Zhang, Shihua Wu, Facile synthesis of porous α-Fe_2O_3 nanorods and their application in ethanol sensors, *Journal of Physical Chemistry C* 112 (2008) 17804–17808.

[11]. Huixiang Tang, Mi Yan, Hui Zhang, Shenzhong Li, Xingfa Ma, Mang Wang, Deren Yang, A selective NH_3 gas sensor based on Fe_2O_3-ZnO nanocomposites at room temperature, *Sensors and Actuators B* 141 (2006) 910-915.

[12]. X.G. Wen, S.H. Wang, Y. Ding, Z.L. Wang, S.H. Yang, Controlled growth of large-area, uniform, vertically aligned arrays of α-Fe_2O_3 nanobelts and nanowires, *Journal of Physical Chemistry B* 109 (2005) 215-220.

[13]. Hao Liu, Guoxiu Wang, Jinsoo Park, Jiazhao Wang, Huakun Liu, Chao Zhang, Electrochemical performance of α-Fe_2O_3 nanorods as anode material for lithium-ion cells, *Electrochimica Acta* 54 (2009) 1733-1736.

[14]. Fenghua Zhang, Heqing Yang, Xiaoli Xie, Li Li, Lihui Zhang, Jie Yu, Hua Zhao, Bin Liu, Controlled synthesis and gas-sensing properties of hollow sea urchin-like α-Fe_2O_3 nanostructures and α-Fe_2O_3 nanocubes, *Sensors and Actuators B* 141 (2009) 381-389.

[15]. M.F. Casula, Y.W. Jun, D.J. Zaziski, E.M. Chan, A. Corrias, A.P. Alivisatos, The concept of delayed nucleation in nanocrystal growth demonstrated for the case of iron oxide nanodisks, *Journal of American Chemistry Society* 128 (2006) 1675-1682.

[16]. G. Neri, A. Bonavita, S. Galvagno, P. Siciliano, S. Capone, CO and NO_2 sensing properties of doped-Fe_2O_3 thin films prepared by LPD, *Sensors and Actuators B* 82 (2002) 40-47.

[17]. E.T. Lee, G.E. Jang, C.K. Kim, D.H. Yoon, Fabrication and gas sensing properties of α-Fe_2O_3 thin film prepared by plasma enhanced chemical vapor deposition (PECVD), *Sensors and Actuators B* 77 (2001) 221-227.

[18]. M.S. Tong, G.R. Dai, D.S. Gao, Surface modification of oxide thin film and its gas-sensing properties, *Applied Surface Science* 171 (2001) 226-230.

[19]. S.Y. Wang, W. Wang, W.Z. Wang, Z. Jiao, J.H. Liu, Y.T. Qian, Characterization and gas-sensing properties of nanocrystalline iron (III) oxide films prepared by ultrasonic spray pyrolysis on silicon, *Sensors and Actuators B* 69 (2000) 22-27.

[20]. L.P. Zhu, H.M. Xiao, X.M. Liu, S.Y. Fu, Template-free synthesis and characterization of novel 3D urchin-like α-Fe_2O_3 superstructures, *Journal of Material Chemistry* 16 (2006) 1794-1797.